The role of G protein subunit β1

in skeletal development

Thesis for Doctor of Philosophy

RUENGSINPINYA LERDLUCK

Osaka University Graduate School of Dentistry
Course for Oral Science
Department of Molecular and Cellular Biochemistry

Supervisor: Professor Riko Nishimura

September, 2021

Table of Contents

Introduction

Bone tissues function as principal support and stability for the body with the flexible encouragement from the cartilage. Additionally, bone tissues are essential for calcium and phosphate homeostasis, and functions as a harboring of bone marrow and blood cells. During skeletal development, bone tissues require two types of ossification; intramembranous and endochondral ossification [1,2]. Intramembranous ossification occurs in craniofacial bones as well as the lateral part of clavicles. These bones are directly formed by osteoblasts which differentiate from mesenchymal cells [3]. Some osteoblasts are surrounded by mineralized bone matrices and differentiate into osteocytes which contribute to maintain bone homeostasis with osteoblasts and osteoclasts [3,4]. In contrast, endochondral ossification is responsible for the longitudinal growth at each end of developing long bones of the limbs, basal part of the skull, vertebrae, ribs and medial part of clavicles. The endochondral ossification requires multiple steps of chondrocyte differentiation that serves the cartilage template before being replaced by bone [5–7].

For endochondral ossification, mesenchymal cells concentrate and start

differentiating into chondrocyte precursors and resting chondrocytes. The resting chondrocytes grow with proliferation and form well-arranged columns [5,7]. The proliferating chondrocytes undergo maturation with the synthesis of cartilage extracellular matrix (ECM) including type II collagen (Col2) and aggrecan, and then differentiate into prehypertrophic chondrocytes [8]. The prehypertrophic chondrocytes highly express Indian hedgehog (Ihh) and PTH/PTHrP receptor (PPR) as well as Runt-related transcription factor 2 (Runx2) and a zinc finger-containing transcription factor Osterix/Sp7 [9]. Ihh positively stimulates PTHrP which inhibits the transition from prehypertrophic to hypertrophic chondrocytes through the PPR [10]. However, Runx2 and Osterix promote the full progression of hypertrophic chondrocyte differentiation as crucial transcription factors for ossification [11–15]. The hypertrophic chondrocytes produce type X collagen (Col10), and subsequently inducing matrix metalloproteinase 13 (Mmp13) which is required for normal removal of transverse septa to restructure the collagen matrix [16,17]. Later, the apoptosis of these hypertrophic chondrocytes occurs following by the vascular invasion into the vacant lacunae [18]. Eventually, growing cartilage template is systematically replaced by bone tissues [18]. The impairment of these ossifications affects normal skeletal

development and cause disproportionate short stature shown in skeletal dysplasia [19–21].

Heterotrimeric guanine nucleotide-binding proteins (G proteins), which are essential mediators for signal transduction, play important roles in broad range of biological events including skeletal development, bone homeostasis, and its dysfunction leads to bone diseases [21,22]. G proteins are composed of three subunits, α, β, and γ with high affinity in coupling with G protein-coupled receptors (GPCRs) at the inner surface of the plasma membrane in the absence of stimulation. Once GPCRs are activated by external stimuli such as growth factors, cytokines, hormones, and neurotransmitters, they induce conformational change in the Gα subunits to exchange guanosine diphosphate (GDP) for guanosine triphosphate (GTP) [23]. This leads to the reversible dissociation of Gα from Gβγ subunits in the receptor complex, and consequently activated Gα and Gβγ subunits mediate intracellular signals to downstream effector proteins. The signals from Gα and Gβγ subunits are terminated by the GTP hydrolases (GTPases) activity that hydrolyzes the bound GTP to GDP and reassociation of Gα and GDP respectively.

Gα has been reported to modulate adenylyl cyclases, cAMP generation,

protein kinase A activation (PKA) and WNT–β-catenin signaling [24–27]. Additionally, Gβγ directly regulate diverse effectors, including calcium and potassium ion channels, adenylyl cyclase 2, β-adrenergic receptor kinase 1, phospholipase C-β2, and phosphoinositide 3-kinases [28,29]. Although the functional Gβγ unit is operated by both Gβ and Gγ subunits, Gβ and Gγ deletions in mice exhibited different phenotypes [30–33], suggesting the distinct physiological functions between Gβ and Gγ subunits.

G protein subunit β1 (GNB1/Gβ1) is a key component in G protein signaling [23], and GNB1 disruptions have been associated to malfunction of GPCR downstream targets [34,35]. The mutations of *GNB1* gene usually cause global developmental delays, neurodevelopmental disability, intellectual disability, hypotonia, seizure, ophthalmological anomalies and persistent growth delays [36–38]. Additionally, human *GNB1* mutations are correlated with carcinogenesis such as leukemia [39], clear-cell renal cell carcinoma [40] and inflammatory responses including cutaneous mastocytosis [41]. GNB1 has been also reported to negatively regulate the activation of NLRP3 inflammasome that involved in the pathogenesis of several inflammatory diseases [42]. Besides, it is reported that *Gnb1*-deficient mice demonstrate growth retardation and

sometimes exhibit severe neurodevelopmental defects including neural tube defects (NTD) without calvaria formation [34]. Therefore, these reports suggest that GNB1 is involved in skeletal development. However, how GNB1 regulates skeletogenesis has not been investigated yet.

In this study, I assessed *Gnb1*-knockout (KO) mice to reveal the role of GNB1 in skeletal development. *Gnb1*-KO mice showed shortened limbs with decreased ossifying zone of long bones and vertebra compared with wild-type (WT) littermates. Additionally, the expression of *Col10a1* and *Mmp13*, late stage markers of endochondral ossification, was markedly decreased in *Gnb1*-KO mice. These results were consistent to the delayed endochondral ossification observed in the skeletal structure of *Gnb1*-KO mice. Furthermore, the chondrocyte proliferation was intact in *Gnb1*-KO mice. On the contrary, osteoblast maturation and function were not interfered in the deletion of *Gnb1*. Taken together, these results indicate that GNB1 is a significant regulatory component for, at least, the late stage of endochondral ossification.

Materials and Methods

Mice and Genotyping

Gnb1-heterozygous mutant (*Gnb1*+/−, C57BL/6 background) mice were generated by previous study from the disruption of *Gnb1* gene in the first intron by a gene trap insertion [34]. *Gnb1*+/− mice were viable and fertile and showed no visible phenotypic change compared with wild-type (WT) littermates. Homozygous *Gnb1*-KO (*Gnb1*−/−) mice were obtained by mating *Gnb1*+/− mice. To determine mouse genotypes, genomic DNA was prepared from the tail and used as the template for polymerase chain reaction (PCR). Primer sets used for genotyping were primer 1 (5` CACTGGCTCTCTTTCTACCCGAAT 3`) and primer 3 (5` ACTCAGGAGGCAGAAGCAGA 3`) for the WT allele and primer 1 and primer 2 (5` ACCTGAAATGACCCTGTGCCTTAT 3`) for the mutant allele, producing 257 bp and 497 bp PCR fragments respectively. KOD FX Neo (Toyobo, Osaka, Japan) was used for PCR reactions. After denaturing at 94ºC for 2 min, the PCR conditions were cycled 32 times at 98ºC for 10 sec, 60ºC for 30 sec, and 68ºC for 60 sec. The Osaka University Institute Animal Experiment Committee approved all animal studies performed in conformity with regulatory guidelines.

In situ hybridization (ISH)

The fixation of tibias was performed in 4% paraformaldehyde (PFA) in phosphate buffered saline (PBS) overnight at 4°C and embedded in paraffin for preparing 5 μm sliced sections. The sections were deparaffinized and hybridized with chondrocyte gene-specific DIG-labelled RNA probes. An alkaline phosphatase-conjugated anti-DIG antibody (Roche, Mannheim, Germany) was used to detect the signals at a 1:2,500 (v/v) dilution. The color was developed by a NBT/BCIP color development substrate solution (Roche) at room temperature. All steps were carefully performed in RNase-free conditions. The *Gnb1* probe (nucleotides 2194–2742 in NM_008142.4) was amplified using specific primers (sense primer: 5` GGGTTTCCTGTGAAGTTGGA 3`, anti-sense primer: 5` GCAAAAGGCTGTTCTTCCAG 3`) and subcloned into the pGEM®-T Easy vector (Promega, WI, USA). Plasmid vectors containing fragments of *Col2a1* (405 bp), *Col10a1* (637 bp), *Ihh* (579 bp), *Ppr* (779 bp), *Mmp13* (639 bp), *Runx2* (634 bp) and *Osterix* (1,315 bp) were linearized using EcoRI (*Col2a1* and *Ihh*), or BamHI (*Col10a1*, *Mmp13*, *Runx2*, and *Osterix*) or XbaI (*Ppr*) respectively [15,43]. The antisense RNA probes labelled digoxigenin (DIG) were generated with SP6 (*Ppr*), T3 (*Col2a1*, *Runx2*, and *Osterix*) or T7 (*Gnb1*, *Col10a1*, and *Mmp13*) RNA

polymerase using the DIG RNA Labeling kit (Roche) following the manufacturer's instructions [15,43].

Histology and Immunohistochemistry

The fixation of tibias was performed in 4% PFA–PBS overnight at 4°C. Following dehydration with ethanol, the tibias were embedded in paraffin, and prepared into 5 μm sections for histological analyses. The hematoxylin and eosin (H&E) and von Kossa staining were performed after deparaffinization. Mineralization was visualized by von Kossa staining. For von Kossa staining, deparaffinized sections were serially rehydrated by immersion in graded ethanol. After staining with 5% silver nitrate at room temperature under the exposure to natural light for 30 min, the sections were wash with PBS and 5% sodium thiosulfate pentahydrate. The Kernechtrot staining was then performed for a counterstaining after the von Kossa staining.

To visualize the expression of *lacZ* gene by X-gal staining, fixation of hindlimbs was performed with 0.2% glutaraldehyde for 30 min. Next, hindlimbs were stained with X-gal (Wako, Osaka, Japan), PBS containing 5 mM K3Fe(CN)6, 5 mM K4Fe(CN)6, 2 mM MgCl2, 0.02% NP-40, and 1 mg/ml X-gal, and fixed

again. After embedding of hindlimb in paraffin, 10 μm sections were prepared as described previously [34].

For 5-ethynyl-2'-deoxyuridine (EdU) labeling, 100 μl of 10 mM EdU labeling solution per 10 g of mouse body weight was intraperitoneally injected into pregnant mice. After injection for 1 h, the tibias from the harvested embryos were prepared for paraffin sections. Then, detection of EdU-positive cells was performed using the Click-iT™ Plus Edu Alexa Flour™ 555 Imaging kit (Invitrogen, Oregon, USA). The ratio of EdU-labeled chondrocytes relative to the total number of chondrocytes was calculated to quantify the cell proliferation.

For immunohistochemistry, deparaffinized sections were rehydrated with graded ethanol and antigen retrieval was performed using 5% hyaluronidase in PBS for 30 min at 37°C, followed by blocking with 1% BSA in PBS containing 0.05% sodium azide for 1 h. Sections were incubated in primary antibodies using the following antibodies: anti-Col2 (#7050; Chondrex, WA, USA) at a 1:1,000 (v/v) dilution; anti-Col10 (#LSL-LB-0092; Cosmo Bio, Tokyo, Japan) at a 1:500 (v/v) dilution; and anti-Mmp13 (#ab39012; Abcam, Cambridge, UK) at a 1:200 (v/v) dilution at 4°C overnight. After washing with PBS, sections were then incubated for 1 h with secondary antibodies using Goat anti-rabbit IgG (H+L) Alexa Fluor™

Plus 555 (Invitrogen) at a 1:500 (v/v) dilution for Col10 and Mmp13, and Goat anti-mouse IgG (H+L) Alexa Fluor™ Plus 555 (Invitrogen) at a 1:500 (v/v) dilution for Col2. The DFC7000 T digital camera (Leica, Wetzlar, Germany) and DM4B microscope (Leica) were used to acquire the images.

Skeletal preparation

After the skin and internal organs from E15-15.5 mice were removed, the embryos were fixed in 95% ethanol overnight. Skeletons were stained with 0.15% Alcian blue overnight. After dehydration with 100% ethanol and immersion with 1% potassium hydroxide (KOH), bone tissues were stained with 0.002% Alizarin red. Tissues were sequentially cleared in 1% KOH and stored in 100% glycerol.

Primary culture of osteoblasts

The calvaria derived primary osteoblasts were obtained from E17.5 mice by sequential digestion with 0.1% collagenase (Wako) containing 0.2% dispase (ThermoFisher scientific, NY, USA) at 37°C. Osteoblasts were collected from dispersions and then centrifuged for 5 min at 1,500g After removing of the supernatant, the pellet was resuspended and osteoblasts were cultured in α-

MEM medium (Sigma-Aldrich, MO, USA) supplemented with 10% fetal bovine serum (FBS) (Nichirei Bioscience, Tokyo, Japan) and penicillin-streptomycin-glutamine. The primary osteoblasts were cultured to confluence in osteogenic induction medium (α-MEM containing 10% FBS, 50 μg/ml ascorbic acid, and 5 mM β–glycerophosphate) with or without treatment with 100 ng/ml BMP2 (Wako) for 6 days to determine osteoblast differentiation and function. To detect the mineralization of bone matrices, cell cultures were washed with PBS, fixed in 4% PFA–PBS and then stained with Alizarin red S.

Reverse transcriptase quantitative polymerase chain reaction (RT-qPCR)

Total RNAs were harvested directly from hindlimbs or primary osteoblast cultures using Nucleospin RNA Plus (Macherey-Nagel, Düren, Germany) and were denatured at 65°C for 5 min. Then, cDNA was synthesized from total RNA with ReverTra Ace qPCR RT Master Mix (Toyobo). For quantification of mRNA, relative transcript mRNA levels were analyzed by real-time PCR reaction using the THUNDERBIRD SYBR qPCR Mix (Toyobo) in a 20 μl reaction volume on 96-well plates with the ABI Step One Plus real-time PCR system (Applied Biosystems, CA, USA). The amount of target mRNA expression was normalized

to that of *β-actin* mRNA expression. Relative mRNA expression levels were calculated using the comparative CT method. Primer sets used are listed in Table 1.

Statistical analyses

The unpaired two-tailed Student's *t*-test was used to analyze the comparisons of two groups. The two-way ANOVA followed by Bonferroni *post hoc*-test was used to analyze the comparisons of multiple groups. p values < 0.05 were considered significant. Statistical analyses were performed by Graphpad Prism 7 or Microsoft Excel software. All data are provided as mean ± standard error of the mean (SEM).

Results

Gnb1 is widely expressed in osseous tissue

Previous study reported that *Gnb1* is highly expressed in cranial neural plates, neural tubes, spinal cords, and limb buds [34]. I first determined the *Gnb1* expression by assessing LacZ expression, because *Gnb1* gene was disrupted by a gene trap insertion with the presence of β-*galactosidase* providing a visual assay of LacZ activity related to *Gnb1* expression in *Gnb1*-KO mice [34]. To study the *Gnb1* expression in osseous tissue, a murine bone tissue survey using *Gnb1*+/− embryos at embryonic day (E) 15.5 was performed by X-gal staining. X-gal staining preliminarily revealed that osseous tissue including cartilage and perichondrium highly expressed *Gnb1* (Fig. 1A). To confirm the results, *in situ* hybridization analysis for *Gnb1* in E15.5 mice was performed and the results consistently showed ubiquitous expression of *Gnb1* in osseous tissue (Fig. 1B). These results suggest that there is a possibility that GNB1 might contribute to skeletal development.

Dwarfism and shortened limbs are manifested in *Gnb1*-KO mice

The study of *Gnb1*-KO embryos previously reported the NTD with no calvaria formation and manifested dwarfism, suggesting an involvement of GNB1 in skeletogenesis [34]. Thus, the analysis of the skeletal structure in *Gnb1*-KO mice was performed to further examine the role of GNB1 in skeletal development. The deficiency of *Gnb1* causes embryonic or neonatal lethality 2 days after birth [34], I therefore assessed the skeletal phenotypes from *Gnb1*-KO embryos at E15.5 by whole mount skeletal preparation. In this study, 85% of E15.5 *Gnb1*-KO embryos exhibited calvaria formation, while 15% of *Gnb1*-KO embryos exhibited no calvaria formation (Fig. 2A). *Gnb1*+/− embryos showed no visible phenotypic change compared with WT littermates (Fig. 2B). However, both *Gnb1*-KO embryos with and without calvaria formation similarly exhibited dwarfism including shortened limbs compared with their WT littermates (Fig. 2B). I accordingly focused on *Gnb1*-KO embryos with calvaria formation for further study.

Deletion of GNB1 results in impaired skeletal development

To precisely determine whether GNB1 engages in skeletogenesis, the architecture of cartilage and bone tissues was analyzed in *Gnb1*-KO mice by

performing whole mount skeletal preparation. Compared to their WT littermates, *Gnb1*-KO embryos showed dwarfism, shortening of limbs, less mineralized areas in vertebra and long bones (Fig. 3A). Moreover, *Gnb1*-KO embryos also showed less mineralization in parietal bones (Fig. 3B). Additionally, impaired ossification and bent clavicles were exhibited in *Gnb1*-KO embryos (Fig. 3B). Furthermore, the ossifying zone of vertebra and long bones was reduced with the shortened forelimbs and hindlimbs in *Gnb1*-KO embryos (Fig. 3B). Quantitative analysis of clavicle and limb length confirmed the significant shortening of clavicle, femur, and tibia in *Gnb1*-KO embryos compared with their WT littermates (Fig. 3C). Taken together, these results confirmed that GNB1 plays a role in skeletal development and the deletion of GNB1 causes an impairment in both of endochondral and intramembranous ossification.

***Gnb1*-KO mice show a delayed endochondral ossification in the late stage**

To investigate the specific stage of endochondral bone formation disrupted by *Gnb1* deficiency *in vivo*, H&E staining, von Kossa staining, and *in situ* hybridization were performed in tibias at E15.5. H&E staining analysis exhibited that the tibia of *Gnb1*-KO embryos was shorter and thinner than that WT

littermates (Fig. 4A). WT embryos showed that the developing chondrocytes in the growth plate were well-organized with the space indicating a vascular invasion (Fig. 4A and B). However, *Gnb1*-KO embryos displayed a reduced hypertrophic chondrocyte zone and delayed vascularization (Fig. 4A and B). It can be speculated that delayed chondrocyte hypertrophy is responsible for the remarkable shortening of long bones and referring to the retardation of endochondral ossification in *Gnb1*-KO embryos. In agreement with this speculation, von Kossa staining analysis showed the decreased staining intensity and area in tibias of *Gnb1*-KO embryos than in those of WT littermates (Fig. 4A). Taken together, these results indicate that *Gnb1* deficiency causes the impaired chondrocyte differentiation and the less ossification in bone tissues.

Deletion of GNB1 leads to an impairment of *Col10a1* and *Mmp13* expression pattern in bone tissues.

Next, to determine which stage of chondrocyte differentiation is impaired in *Gnb1*-KO mice, I analyzed gene expression of stage-specific chondrocyte markers by performing *in situ* hybridization using E15.5 *Gnb1*-KO mice. The results showed a similar expression pattern of *Col2a1*, an early chondrogenic

marker gene for proliferation, in both *Gnb1*-KO and WT littermates (Fig. 4A) resembling a normal proliferating and pre-hypertrophic chondrocyte zone shown in H&E staining (Fig. 4A). Nevertheless, expression pattern of *Col10a1*, a marker of hypertrophic chondrocytes, was not divided into both sides of the hypertrophic zone in *Gnb1*-KO embryos as it shown a separation in WT littermates, but located at the center of bone (Fig. 4A). Moreover*, Mmp13* expression*,* another late hypertrophic marker of chondrogenesis, was remarkably decreased in *Gnb1*-KO embryos (Fig. 4A). On the other hand, expression of *Runx2,* which is an essential transcription factor for bone formation, osteoblastogenesis, and hypertrophy of chondrocytes [11,12,44,45] and specifically expressed in pre-hypertrophic and hypertrophic chondrocytes [11], was expressed at similar levels in *Gnb1*-KO mice compared with WT littermates. Furthermore, expression of *Osterix*, which is an indispensable transcription factor for bone formation, osteoblastogenesis, and the late stage of endochondral ossification [14,15,46], and specifically expressed in osteoblasts and pre-hypertrophic chondrocytes [15], was unaffected in *Gnb1*-KO embryos (Fig. 4A). Additionally, expression of *Ihh* and *Ppr*, which are specific markers of pre-hypertrophic chondrocytes, was intact in *Gnb1*-KO mice (Fig. 4A). Therefore, these data indicated that chondrocyte differentiation to the early

hypertrophic stage is intact whereas the terminal differentiation of chondrocytes is delayed in *Gnb1* deficiency.

Gnb1 **deficiency down-regulates the** ***Col10a1*** **and** ***Mmp13*** **expression in hypertrophic chondrocytes**

To confirm the expression pattern of Col2, Col10, and Mmp13 in tibia of *Gnb1*-KO mice, I performed a tissue survey using immunohistochemistry with their specific antibodies. The Col2-positive zone was not altered in *Gnb1*-KO mice (Fig. 5A), whereas a shorter Col10-positive zone was observed in *Gnb1*-KO embryos than that in WT littermates, indicating the delayed expression of Col10 (Fig. 5A). Moreover, Mmp13-positive zone was almost not observed in *Gnb1*-KO embryos (Fig. 5A).

To further confirm the altered expression of Col10, and Mmp13 in bone tissues, I quantitatively analyzed the gene expression of chondrocyte differentiation markers in bone tissues of *Gnb1*-KO embryos by performing RT-qPCR. The *Col2a1, Runx2*, *Osterix*, *Ihh*, *Ppr*, and *Pthrp* mRNA level was not significantly changed in *Gnb1*-KO embryos compared with WT littermates (Fig. 5B). However, compared with WT littermates, mRNA expression of *Col10a1* and

Mmp13 was significantly decreased in *Gnb1*-KO mice (Fig. 5B). These results further indicate the maturation of hypertrophic chondrocytes is impaired in *Gnb1*-KO mice.

Collectively, the *in situ* hybridization analyses were consistent to immunohistochemical and RT-qPCR experiments. Thus, these findings supported that GNB1 involves in the late stage of endochondral ossification by controlling *Col10a1* and *Mmp13* expression.

The chondrocyte proliferation is intact in *Gnb1* deficiency

To examine whether the defect of chondrocyte proliferation is involved in a dwarfism and significant shortening of long bones in *Gnb1*-KO mice, *in vivo* EdU incorporation assays were performed in E15.5 *Gnb1*-KO embryos. According to the quantitative analyses based on the stained slices from *Gnb1*-KO embryos and WT littermates, there was no significant alteration in the ratio of EdU-positive proliferating chondrocyte numbers to total DAPI positive nuclei, indicating an intact chondrocyte proliferation in *Gnb1*-KO mice (Fig. 6A and B). These data indicated that defective endochondral ossification observed in *Gnb1*-KO mice resulted from the impairment of chondrocyte differentiation, but not from

the impairment of chondrocyte proliferation.

Osteoblast differentiation and bone formation are not interfered in *Gnb1*-KO-derived osteoblasts

As dwarfism and significant shortening with malformation phenotype of clavicle were displayed in *Gnb1*-KO embryos (Fig. 3A, B and C), I therefore examined the consequences of the *Gnb1* deficiency to osteoblastogenic and calcifying activities. To address this, the primary osteoblasts were isolated from calvariae of *Gnb1*-KO and WT littermates and were cultured in the absence or presence of BMP2. In the osteoblast culture with BMP2, BMP2 induces osteoblast differentiation and function. The staining results were identical in both *Gnb1*-KO and WT mice derived osteoblast cultures (Fig. 7A), suggesting the intact differentiation and mineralization of osteoblasts in *Gnb1*-KO embryos.

To further characterize the role of GNB1 during intramembranous ossification, RT-qPCR analyses were performed for osteoblast differentiation markers at different stages. *Col1a1*, encodes collagen type I alpha 1 chain, is an early stage marker of osteoblast differentiation [3]. *Alkaline phosphatase* (*Alp*), a dephosphorylation enzyme for mineralization, is a marker of osteoblast activity

[3,47,48]. *Osteocalcin* (*Ocn*), which is synthesized by mature osteoblasts, is a late stage marker of osteoblast differentiation [45]. RT-qPCR analyses from *Gnb1*-KO osteoblast cultures in the absence or presence of BMP2 also presented an unchanged mRNA expression of *Col1a1, Alp*, and *Ocn* compared to their WT littermates (Fig. 7B). These results indicated that *Gnb1* seems to be independent from regulation of osteoblast differentiation and function, and the absence of calvaria formation observed in *Gnb1*-KO mice is not resulted from the impairment of osteoblast differentiation and function.

Discussion

Although the involvement of GNB1 in skeletal development was implied in previous genetic studies [34,36–38], the precise role of GNB1 in skeletal development was still elusive. In this study, I found that impaired endochondral ossification is accountable for dwarfism and shortened limb phenotypes observed in *Gnb1*-KO mice in presence or absence of calvaria formation. Expression of *Col10a1* and *Mmp13*, late stage markers of chondrocyte hypertrophy in endochondral ossification, was reduced in *Gnb1*-KO mice from the analyses of *in situ* hybridization and RT-qPCR. In accordance with this, the reduction of chondrocyte hypertrophy and calcification were also presented in tibias of *Gnb1*-KO mice, whereas chondrocyte proliferation appeared intact. However, osteoblast differentiation and activities in *Gnb1*-KO mice seemed to be intact. Taken together, these results demonstrate that GNB1 functions, at least in part, as a positive regulator for the late stage of endochondral ossification.

According to the report of neurodevelopmental disorders and growth delays in human *GNB1* mutations [36–38], these neurodevelopmental disorders are developed by the impairment of GNB1 function in neurons [34]. However, the

association of *GNB1* mutations to growth retardation has not been analyzed. In this study, the delay of endochondral ossification in the absence of GNB1 indicates that the *GNB1* mutation-related growth delay is caused by the impairment of endochondral ossification, even though the involvement of an abnormal nervous system is not excluded.

I clearly indicate, in this study, that the significant reduction in *Col10a1* and *Mmp13* expression was presented in *Gnb1*-KO mice. During endochondral ossification, *Col10a1* and *Mmp13* expression is regulated by Runx2 and/or Osterix [15,49]. Furthermore, *Runx2*-KO and *Osterix*-KO mice display an impaired endochondral ossification [15,45]. Nevertheless, *Gnb1*-KO mice showed the normal *Runx2* and *Osterix* expression. The function of Runx2 is intact in *Gnb1*-KO mice because Runx2 is critical to induce Osterix expression in developing chondrocytes as well as osteoblasts [15]. Therefore, Runx2 and Osterix would not account for the decreased expression of *Col10a1* and *Mmp13* in *Gnb1*-KO mice, and other factors are involved in these expression and dwarf phenotype in *Gnb1*-KO mice.

The study of crystal structures of heterotrimeric G protein for understanding how GNB1 interacts with protein partners in the transmission cascade reported

that mutations in *GNB1* gene affect Gβ residues and interrupt the interrelation between Gα subunits, Gγ subunits, or G protein signaling downstream effectors [28,35,37,50]. Additionally, the alterations of GNB1 function in *GNB1* mutations can cause both loss and gain of function [35–37]. GNB1 loss-of-function is due to defective function of mutated GNB1 to form Gβγ dimer resulting in the deficiency of GPCR-induced G protein activations [37,51]. However, the gain-of-function in engaging Gβγ effectors from several GNB1 mutations are reported due to the inappropriate or constitutive activation of G protein downstream signaling cascades, leading to a clonal neoplasm in diverse human tumors [35,36]. The constitutive active *GNB1* mutations increase the activation of PI3K-AKT- mTOR and ERK signaling pathways [35,52]. On the other hand, *Gnb1*-KO mice showed a reduction of ERK phosphorylation in neural progenitor cells [34]. During skeletal development, ERK and AKT signaling pathways are the key signaling pathways involved in hypertrophic differentiation of chondrocytes [53–55], and contribute to the regulation of *Col10a1* and *Mmp13* expression [55–58]. Therefore, GNB1 deficiency is possibly responsible for delayed endochondral ossification through the interference of ERK and/or AKT signaling pathways that down-regulate *Col10a1* and *Mmp13* expression. Further investigation on the

correlation of GNB1 and ERK and AKT signaling pathways in endochondral ossification is indispensable for further insights.

Some *Gnb1*-KO mice showed no calvaria formation while osteoblast activities were intact in *Gnb1*-KO mice. The lack of skull ossification has been reported in gene mutations associated with not only ossification, but also the neural tube closure [59]. The process of fetal head formation is originated from mesoderm and cranial neural crest after neurulation [60], indicating that the interruption of neural tube closure can interfere normal calvaria formation. The interruption of neural tube closure is reported to result from the disruption of actin cytoskeleton [61]. Indeed, the impaired actin organization in neuroepithelium is reported in *Gnb1*-KO mice [34], suggesting that the absence of calvaria formation in *Gnb1*-KO mice is predominantly resulted from a defective embryonic neurogenesis with disruption of cranial neural tube closure.

The NTD with the absence of calvaria formation is not always manifested in *Gnb1*-KO mice. Interestingly, the NTD with the absence of calvaria formation are observed in many mutant mice with variation of the penetrance [62,63]. These studies indicate that the variation of penetrance of NTD including *Gnb1*-KO mice is dependent on multiple factors such as gene functions and environments.

Further study is required for understanding the mechanism of penetrance of NTD.

The clavicle shortening and deformation in *Gnb1*-KO mice indicated that intramembranous ossification was also impaired in *Gnb1*-KO mice. However, it was not caused by an impairment of osteoblast differentiation and function. Previous study reported that *Gnb1* is highly expressed in the cranial neural plate and neural tube [34] and widely distributed throughout the brain [30,34]. Therefore, the absence of GNB1 may affect the nervous system including pituitary functions which involve in somatic growth [64]. Indeed, mice lacking one *gna*11 allele, a subunit of Gq/11 family in Gα subunits, in the nervous system showed defective anterior pituitary functions with growth retardation [65]. Thus, one possibility accordingly reasoned for the defective intramembranous ossification in clavicle of *Gnb1*-KO mice is resulted from the impaired pituitary function.

Other G protein subunits are also reported in association of skeletal development [21], and G protein subunit alpha isoforms short (*GNAS*) gene, which encodes Gαs, are well analyzed [21,25–27,66]. The mutations of *GNAS* gene cause skeletal abnormalities, and *GNAS* gain-of-function mutations cause fibrous dysplasia (FD) in McCune-Albright Syndrome (MAS) [67–69] while *GNAS*

loss-of-function mutations cause progressive osseous heteroplasia (POH) and Albright's hereditary osteodystrophy (AHO) [70,71]. *In vivo* studies using chondrocyte specific *Gnas*-KO mice showed that GNAS negatively regulates chondrocyte differentiation. Histological studies reported the remarkable shortening of proliferating chondrocyte zone with an accelerated rate of differentiation into hypertrophic chondrocytes, whereas the hypertrophic chondrocyte zone was not affected, indicating premature growth plate development in *Gnas* deficiency [72,73]. Furthermore, ectopic cartilage formation with the expression of hypertrophic chondrocyte markers was developed in *Gnas*-KO mice [72–74]**.** In this study, chondrocytes can differentiate until the late stage of endochondral ossification without any ectopic cartilage formation in the absence of GNB1. Therefore, GNB1 would regulate the late stage of endochondral ossification in a GNAS independent manner.

In summary, these *in vivo* evidences underline the requisite of GNB1 in skeletal development. Therefore, these findings contribute to the understanding of GNB1 role in skeletal development which will enhance a novel knowledge of growth related phenotypes in *GNB1* mutations and may allow to develop effective and potent therapeutic options for GNB1 associated growth retardation.

Acknowledgements

I would like to express my deep and sincere gratitude to my research supervisors, Dr. Riko Nishimura, DDS, PhD, Professor and Chair, as well as Dr. Tomohiko Murakami, PhD, Associate Professor, Department of Molecular & Cellular Biochemistry, Osaka University Graduate School of Dentistry for giving me the opportunity to do research and providing invaluable guidance throughout these research and writing this thesis. It was a great privilege and honor to work and study under their support. I would also like to thank them for their kindness and empathy in my daily life apart from pursuing the research.

My sincere thanks also goes to Dr. Kenji Hata and Dr. Yoshifumi Takahata for guiding me all insight techniques and precious suggestions. In particular, I offer my sincere appreciation for the learning opportunities provided by Dr. Eriko Nakamura.

I cannot express enough thanks to Dr. Yoichiro Iwakura (Tokyo University of Science, Tokyo, Japan) and Dr. Hiroaki Okae (Tohoku University, Sendai, Japan) for providing *Gnb1*+/− mice. Besides, Dr. Noriyuki Tsumaki (Kyoto University, Kyoto, Japan) and Dr. Toshihisa Komori (Nagasaki University Dental

School, Nagasaki, Japan) for providing chondrocyte gene probes for *in situ* hybridization.

My completion of this research could not have been accomplished without the support of my lab mates and Thai friends. Last but not the least, I would like to thank my family for always supporting me spiritually throughout my life.

References

[1] B.R. Olsen, A.M. Reginato, W. Wang, Bone development, Annu. Rev. Cell Dev. Biol. 16 (2000) 191–220. https://doi.org/10.1146/annurev.cellbio.16.1.191.

[2] Z.L. Deng, K.A. Sharff, N. Tang, et al., Regulation of osteogenic differentiation during skeletal development, Front. Biosci. 13 (2008) 2001–2021. https://doi.org/10.2741/2819.

[3] G.S. Stein, J.B. Lian, T.A. Owen, Relationship of cell growth to the regulation of tissue-specific gene expression during osteoblast differentiation, FASEB J. 4 (1990) 3111–3123.

[4] F. Long, Building strong bones: Molecular regulation of the osteoblast lineage, Nat. Rev. Mol. Cell Biol. 13 (2012) 27–38. https://doi.org/10.1038/nrm3254.

[5] H.M. Kronenberg, Developmental regulation of the growth plate, Nature. 423 (2003) 332–336. https://doi.org/10.1038/nature01657.

[6] E.J. Mackie, Y.A. Ahmed, L. Tatarczuch, et al., Endochondral ossification: How cartilage is converted into bone in the developing skeleton, Int. J.

Biochem. Cell Biol. (2008) 46–62. https://doi.org/10.1016/j.biocel.2007.06.009.

[7] K. Hata, Y. Takahata, T. Murakami, R. Nishimura, Transcriptional network controlling endochondral ossification, J. Bone Metab. 24 (2017) 75–82. https://doi.org/10.11005/jbm.2017.24.2.75.

[8] B. De Crombrugghe, V. Lefebvre, R.R. Behringer, et al., Transcriptional mechanisms of chondrocyte differentiation, Matrix Biol. 19 (2000) 389–394. https://doi.org/10.1016/S0945-053X(00)00094-9.

[9] V. Lefebvre, P. Smits, Transcriptional control of chondrocyte fate and differentiation, Birth Defects Res. Part C - Embryo Today Rev. 75 (2005) 200–212. https://doi.org/10.1002/bdrc.20048.

[10] U. Il Chung, E. Schipani, A.P. McMahon, H.M. Kronenberg, Indian hedgehog couples chondrogenesis to osteogenesis in endochondral bone development, J. Clin. Invest. 107 (2001) 295–304. https://doi.org/10.1172/JCI11706.

[11] H. Enomoto, M. Enomoto-Iwamoto, M. Iwamoto, et al., Cbfa1 is a positive regulatory factor in chondrocyte maturation, J. Biol. Chem. 275 (2000) 8695–8702. https://doi.org/10.1074/jbc.275.12.8695.

[12] C.A. Yoshida, H. Yamamoto, T. Fujita, et al., Runx2 and Runx3 are essential for chondrocyte maturation, and Runx2 regulates limb growth through induction of Indian hedgehog, Genes Dev. 18 (2004) 952–963. https://doi.org/10.1101/gad.1174704.

[13] G.S. Stein, J.B. Lian, A.J. Van Wijnen, et al., Runx2 control of organization, assembly and activity of the regulatory machinery for skeletal gene expression, Oncogene. 23 (2004) 4315–4329. https://doi.org/10.1038/sj.onc.1207676.

[14] T. Matsubara, K. Kida, A. Yamaguchi, et al., BMP2 regulates osterix through Msx2 and Runx2 during osteoblast differentiation, J. Biol. Chem. 283 (2008) 29119–29125. https://doi.org/10.1074/jbc.M801774200.

[15] R. Nishimura, M. Wakabayashi, K. Hata, et al., Osterix regulates calcification and degradation of chondrogenic matrices through matrix metalloproteinase 13 (MMP13) expression in association with transcription factor Runx2 during endochondral ossification, J. Biol. Chem. 287 (2012) 33179–33190. https://doi.org/10.1074/jbc.M111.337063.

[16] J. Gu, Y. Lu, F. Li, et al., Identification and characterization of the novel

Col10a1 regulatory mechanism during chondrocyte hypertrophic differentiation, Cell Death Dis. 5 (2014). https://doi.org/10.1038/cddis.2014.444.

[17] M. Inada, Y. Wang, M.H. Byrne, et al., Critical roles for collagenase-3 (Mmp13) in development of growth plate cartilage and in endochondral ossification, Proc. Natl. Acad. Sci. U. S. A. 101 (2004) 17192–17197. https://doi.org/10.1073/pnas.0407788101.

[18] C. Maes, Role and regulation of vascularization processes in endochondral bones, Calcif. Tissue Int. 92 (2013) 307–323. https://doi.org/10.1007/s00223-012-9689-z.

[19] A. Superti-Furga, L. Bonafé, D.L. Rimoin, Molecular-pathogenetic classification of genetic disorders of the skeleton, Am. J. Med. Genet. - Semin. Med. Genet. 106 (2001) 282–293. https://doi.org/10.1002/ajmg.10233.

[20] D. Krakow, D.L. Rimoin, The skeletal dysplasias, Genet. Med. 12 (2010) 327–341. https://doi.org/10.1097/GIM.0b013e3181daae9b.

[21] M. Wu, L. Deng, G. Zhu, Y.P. Li, G protein and its signaling pathway in bone development and disease, Front. Biosci. 15 (2010) 957–985.

https://doi.org/10.2741/3656.

[22] J. Luo, P. Sun, S. Siwko, et al., The role of GPCRs in bone diseases and dysfunctions, Bone Res. 7 (2019). https://doi.org/10.1038/s41413-019-0059-6.

[23] W.M. Oldham, H.E. Hamm, Heterotrimeric G protein activation by G-protein-coupled receptors, Nat. Rev. Mol. Cell Biol. 9 (2008) 60–71. https://doi.org/10.1038/nrm2299.

[24] L.S. Weinstein, S. Yu, D.R. Warner, J. Liu, Endocrine manifestations of stimulatory G protein α subunit mutations and the role of genomic imprinting, Endocr. Rev. 22 (2001) 675–705. https://doi.org/10.1210/er.22.5.675.

[25] S. Zhang, F.S. Kaplan, E.M. Shore, Different roles of GNAS and cAMP signaling during early and late stages of osteogenic differentiation, Horm. Metab. Res. 44 (2012) 724–731. https://doi.org/10.1055/s-0032-1321845.

[26] J.B. Regard, D. Malhotra, J. Gvozdenovic-Jeremic, et al., Activation of hedgehog signaling by loss of GNAS causes heterotopic ossification, Nat. Med. 19 (2013) 1505–1512. https://doi.org/10.1038/nm.3314.

[27] R. Xu, S.K. Khan, T. Zhou, et al., Gαs signaling controls intramembranous

ossification during cranial bone development by regulating both Hedgehog and Wnt/β-catenin signaling, Bone Res. 6 (2018) 1–15. https://doi.org/10.1038/s41413-018-0034-7.

[28] C.E. Ford, N.P. Skiba, H. Bae, et al., Molecular basis for interactions of G protein βγ subunits with effectors, Science. 280 (1998) 1271–1274. https://doi.org/10.1126/science.280.5367.1271.

[29] S.M. Khan, R. Sleno, S. Gora, et al., The expanding roles of Gβγ subunits in G protein-coupled receptor signaling and drug action, Pharmacol. Rev. 65 (2013) 545–577. https://doi.org/10.1124/pr.111.005603.

[30] M. Betty, S.W. Harnish, K.J. Rhodes, M.I. Cockett, Distribution of heterotrimeric G-protein β and γ subunits in the rat brain, Neuroscience. 85 (1998) 475–486. https://doi.org/10.1016/S0306-4522(97)00623-4.

[31] J.H. Zhang, M. Pandey, E.M. Seigneur, et al., Knockout of G protein β5 impairs brain development and causes multiple neurologic abnormalities in mice, J. Neurochem. 119 (2011) 544–554. https://doi.org/10.1111/j.1471-4159.2011.07457.x.

[32] F. Li, S. Ponissery-Saidu, K.K. Yee, et al., Heterotrimeric G protein subunit Gγ13 is critical to olfaction, J. Neurosci. 33 (2013) 7975–7984.

https://doi.org/10.1523/JNEUROSCI.5563-12.2013.

[33] V. Syrovatkina, K.O. Alegre, R. Dey, X.Y. Huang, Regulation, signaling, and physiological functions of G-proteins, J. Mol. Biol. 428 (2016) 3850–3868. https://doi.org/10.1016/j.jmb.2016.08.002.

[34] H. Okae, Y. Iwakura, Neural tube defects and impaired neural progenitor cell proliferation in Gβ1-deficient mice, Dev. Dyn. 239 (2010) 1089–1101. https://doi.org/10.1002/dvdy.22256.

[35] A. Yoda, G. Adelmant, J. Tamburini, et al., Mutations in G protein β subunits promote transformation and kinase inhibitor resistance, Nat. Med. 21 (2015) 71–75. https://doi.org/10.1038/nm.3751.

[36] S. Petrovski, S. Küry, C.T. Myers, et al., Germline de novo mutations in GNB1 cause severe neurodevelopmental disability, hypotonia, and seizures, Am. J. Hum. Genet. 98 (2016) 1001–1010. https://doi.org/10.1016/j.ajhg.2016.03.011.

[37] K. Lohmann, I. Masuho, D.N. Patil, et al., Novel GNB1 mutations disrupt assembly and function of G protein heterotrimers and cause global developmental delay in humans, Hum. Mol. Genet. 26 (2017) 1078–1086. https://doi.org/10.1093/hmg/ddx018.

[38] P. Hemati, A. Revah-Politi, H. Bassan, et al., Refining the phenotype associated with GNB1 mutations: Clinical data on 18 newly identified patients and review of the literature, Am. J. Med. Genet. Part A. 176 (2018) 2259–2275. https://doi.org/10.1002/ajmg.a.40472.

[39] M. Brett, A.H.M. Lai, T.W. Ting, et al., Acute lymphoblastic leukemia in a child with a de novo germline gnb1 mutation, Am. J. Med. Genet. Part A. 173 (2017) 550–552. https://doi.org/10.1002/ajmg.a.38026.

[40] C. Chen, C. Huang, M. Liu, J. Zheng, Downregulation of guanine nucleotide-binding protein beta 1 (GNB1) is associated with worsened prognosis of clear-cell renal cell carcinoma and is related to VEGF signaling pathway, J. B.U.ON. 22 (2017) 1441–1446.

[41] K. Szczałuba, A. Biernacka, K. Szymańska, et al., Novel GNB1 de novo mutation in a patient with neurodevelopmental disorder and cutaneous mastocytosis: Clinical report and literature review, Eur. J. Med. Genet. 61 (2018) 157–160. https://doi.org/10.1016/j.ejmg.2017.11.010.

[42] T. Murakami, L. Ruengsinpinya, E. Nakamura, et al., Cutting edge: G protein subunit β 1 negatively regulates NLRP3 inflammasome activation, J. Immunol. 202 (2019) 1942–1947.

https://doi.org/10.4049/jimmunol.1801388.

[43] M. Yoshida, K. Hata, R. Takashima, et al., The transcription factor Foxc1 is necessary for Ihh-Gli2-regulated endochondral ossification, Nat. Commun. 6 (2015) 1–15. https://doi.org/10.1038/ncomms7653.

[44] F. Otto, A.P. Thornell, T. Crompton, et al., Cbfa1, a candidate gene for cleidocranial dysplasia syndrome, is essential for osteoblast differentiation and bone development, Cell. 89 (1997) 765–771. https://doi.org/10.1016/S0092-8674(00)80259-7.

[45] T. Komori, H. Yagi, S. Nomura, et al., Targeted disruption of Cbfa1 results in a complete lack of bone formation owing to maturational arrest of osteoblasts, Cell. 89 (1997) 755–764. https://doi.org/10.1016/S0092-8674(00)80258-5.

[46] K. Nakashima, X. Zhou, G. Kunkel, et al., The novel zinc finger-containing transcription factor Osterix is required for osteoblast differentiation and bone formation, Cell. 108 (2002) 17–29. https://doi.org/10.1016/S0092-8674(01)00622-5.

[47] J.E. Aubin, F. Liu, L. Malaval, A.K. Gupta, Osteoblast and chondroblast differentiation, Bone. 17 (1995) 77S-83S. https://doi.org/10.1016/8756-

3282(95)00183-E.

[48] E.G. Ellis, B.B. Kathleen, The role of alkaline phosphatase in osteogenesis., Curr. Opin. Orthop. 18 (2007) 444–448. https://doi.org/10.1097/BCO.0b013e3282630851.

[49] Q. Zheng, G. Zhou, R. Morello, et al., Type X collagen gene regulation by Runx2 contributes directly to its hypertrophic chondrocyte-specific expression in vivo, J. Cell Biol. 162 (2003) 833–842. https://doi.org/10.1083/jcb.200211089.

[50] A. V Smrcka, I. Fisher, G-protein βγ subunits as multi-functional scaffolds and transducers in G-protein-coupled receptor signaling, Cell. Mol. Life Sci. 76 (2019) 4447–4459. https://doi.org/10.1007/s00018-019-03275-2.

[51] L. Schultz-Rogers, I. Masuho, F. Pinto e Vairo, et al., Haploinsufficiency as a disease mechanism in GNB1-associated neurodevelopmental disorder, Mol. Genet. Genomic Med. 8 (2020) 1–9. https://doi.org/10.1002/mgg3.1477.

[52] O. Zimmermannova, E. Doktorova, J. Stuchly, et al., An activating mutation of GNB1 is associated with resistance to tyrosine kinase inhibitors in ETV6-ABL1-positive leukemia, Oncogene. 36 (2017) 5985–

5994. https://doi.org/10.1038/onc.2017.210.

[53] M.M. McKay, D.K. Morrison, Integrating signals from RTKs to ERK/MAPK, Oncogene. 26 (2007) 3113–3121. https://doi.org/10.1038/sj.onc.1210394.

[54] V. Ulici, K.D. Hoenselaar, J.R. Gillespie, F. Beier, The PI3K pathway regulates endochondral bone growth through control of hypertrophic chondrocyte differentiation, BMC Dev. Biol. 8 (2008). https://doi.org/10.1186/1471-213X-8-40.

[55] Z. Chen, S.X. Yue, G. Zhou, et al., ERK1 and ERK2 regulate chondrocyte terminal differentiation during endochondral bone formation, J. Bone Miner. Res. 30 (2015) 765–774. https://doi.org/10.1002/jbmr.2409.

[56] T. Matsushita, Y.Y. Chan, A. Kawanami, et al., Extracellular signal-regulated kinase 1 (ERK1) and ERK2 play essential roles in osteoblast differentiation and in supporting osteoclastogenesis, Mol. Cell. Biol. 29 (2009) 5843–5857. https://doi.org/10.1128/mcb.01549-08.

[57] D. Ikegami, H. Akiyama, A. Suzuki, et al., Sox9 sustains chondrocyte survival and hypertrophy in part through Pik3ca-Akt pathways, Development. 138 (2011) 1507–1519.

https://doi.org/10.1242/dev.057802.

[58] M.A. Greene, R.F. Loeser, Function of the chondrocyte PI-3 kinase-Akt signaling pathway is stimulus dependent, Osteoarthr. Cartil. 23 (2015) 949–956. https://doi.org/10.1016/j.joca.2015.01.014.

[59] A.N. Abell, J.A. Rivera-Perez, B.D. Cuevas, et al., Ablation of MEKK4 kinase activity causes neurulation and skeletal patterning defects in the mouse embryo, Mol. Cell. Biol. 25 (2005) 8948–8959. https://doi.org/10.1128/MCB.25.20.8948-8959.2005.

[60] S.W. Jin, K.B. Sim, S.D. Kim, Development and growth of the normal cranial vault: An embryologic review, J. Korean Neurosurg. Soc. 59 (2016) 192–196. https://doi.org/10.3340/jkns.2016.59.3.192.

[61] P. Ybot-Gonzalez, A.J. Copp, Bending of the neural plate during mouse spinal neurulation is independent of actin microfilaments, Dev. Dyn. 215 (1999) 273–283. https://doi.org/10.1002/(SICI)1097-0177(199907)215:3<273::AID-AJA9>3.0.CO;2-H.

[62] M.J. Harris, D.M. Juriloff, Mouse mutants with neural tube closure defects and their role in understanding human neural tube defects, Birth Defects Res. Part A - Clin. Mol. Teratol. 79 (2007) 187–210.

https://doi.org/10.1002/bdra.20333.

[63] M.J. Harris, D.M. Juriloff, An update to the list of mouse mutants with neural tube closure defects and advances toward a complete genetic perspective of neural tube closure, Birth Defects Res. Part A - Clin. Mol. Teratol. 88 (2010) 653–669. https://doi.org/10.1002/bdra.20676.

[64] D. Ray, S. Melmed, Pituitary cytokine and growth factor expression and action, Endocr. Rev. 18 (1997) 206–228. https://doi.org/10.1210/edrv.18.2.0297.

[65] N. Wettschureck, A. Moers, B. Wallenwein, et al., Loss of Gq/11 family G proteins in the nervous system causes pituitary somatotroph hypoplasia and dwarfism in mice, Mol. Cell. Biol. 25 (2005) 1942–1948. https://doi.org/10.1128/MCB.25.5.1942-1948.2005.

[66] A. Sakamoto, M. Chen, T. Nakamura, et al., Deficiency of the G-protein α-subunit Gsα in osteoblasts leads to differential effects on trabecular and cortical bone, J. Biol. Chem. 280 (2005) 21369–21375. https://doi.org/10.1074/jbc.M500346200.

[67] C. Robinson, M.T. Collins, A.M. Boyce, Fibrous dysplasia/McCune-Albright syndrome: Clinical and translational perspectives, Curr.

Osteoporos. Rep. 14 (2016) 178–186. https://doi.org/10.1007/s11914-016-0317-0.

[68] R.D. Chapurlat, P. Orcel, Fibrous dysplasia of bone and McCune-Albright syndrome, Best Pract. Res. Clin. Rheumatol. 22 (2008) 55–69. https://doi.org/10.1016/j.berh.2007.11.004.

[69] M. Riminucci, L.W. Fisher, A. Shenker, et al., Fibrous dysplasia of bone in the McCune-Albright syndrome: Abnormalities in bone formation, Am. J. Pathol. 151 (1997) 1587–1600.

[70] M.A. Levine, T.G. Ahn, S.F. Klupt, et al., Genetic deficiency of the α subunit of the guanine nucleotide-binding protein G(s) as the molecular basis for Albright hereditary osteodystrophy, Proc. Natl. Acad. Sci. U. S. A. 85 (1988) 617–621. https://doi.org/10.1073/pnas.85.2.617.

[71] F.S. Kaplan, E.M. Shore, Perspective: Progressive osseous heteroplasia, J. Bone Miner. Res. 15 (2000) 2084–2094. https://doi.org/10.1359/jbmr.2000.15.11.2084.

[72] M. Bastepe, L.S. Weinstein, N. Ogata, et al., Stimulatory G protein directly regulates hypertrophic differentiation of growth plate cartilage in vivo, Proc. Natl. Acad. Sci. U. S. A. 101 (2004) 14794–14799.

https://doi.org/10.1073/pnas.0405091101.

[73] A. Sakamoto, M. Chen, T. Kobayashi, et al., Chondrocyte-specific knockout of the G protein Gsα leads to epiphyseal and growth plate abnormalities and ectopic chondrocyte formation, J. Bone Miner. Res. 20 (2005) 663–671. https://doi.org/10.1359/JBMR.041210.

[74] H. Castrop, M. Oppermann, D. Mizel, et al., Skeletal abnormalities and extra-skeletal ossification in mice with restricted Gsα deletion caused by a renin promoter-Cre transgene, Cell Tissue Res. 330 (2007) 487–501. https://doi.org/10.1007/s00441-007-0491-6.

Publication list

L. Ruengsinpinya, T. Murakami, E. Nakamura, Y. Takahata, et al., G protein subunit β1 is an important mediator of the late stage of endochondral ossification, *Biochem. Biophys. Res. Commun.* 533 (2020) 90–96. https://doi.org/10.1016/j.bbrc.2020.08.119.

Figures

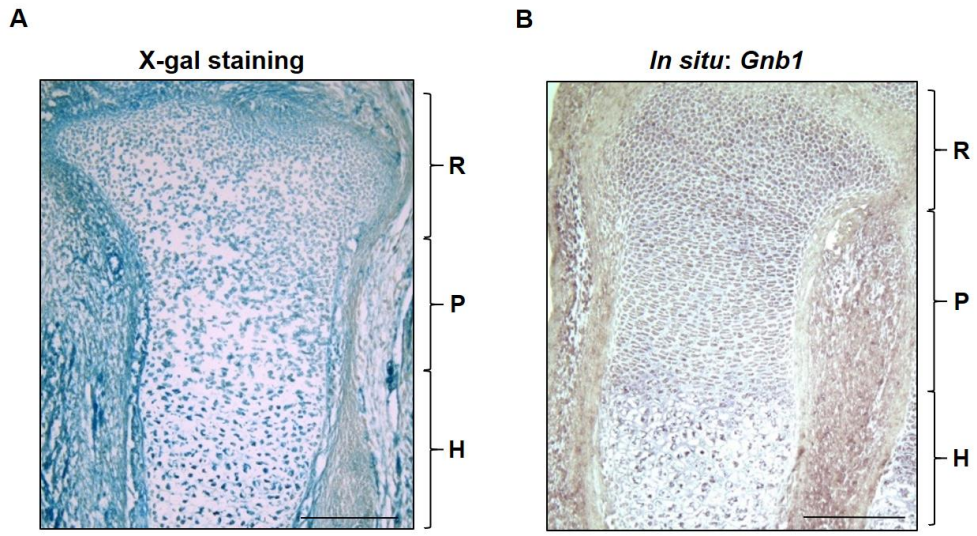

Fig. 1. *Gnb1* expression in osseous tissue.

(A) X-gal staining in developing tibia of E15.5 *Gnb1*-heterozygous embryos.

(B) *In situ* hybridization for *Gnb1* expression in developing tibia of E15.5 WT embryos.

R indicates resting chondrocyte zone, P indicates proliferating chondrocyte zone, and H indicates hypertrophic chondrocyte zone. Scale bar, 200 μm.

A

Offspring genotypes from *Gnb1* heterozygous intercrosses

Genotype	WT	+/-	KO with calvaria formation	KO without calvaria formation
Number of pups	34	57	28	5
Percentage of pups	27%	46%	23% (85%)	4% (15%)

B

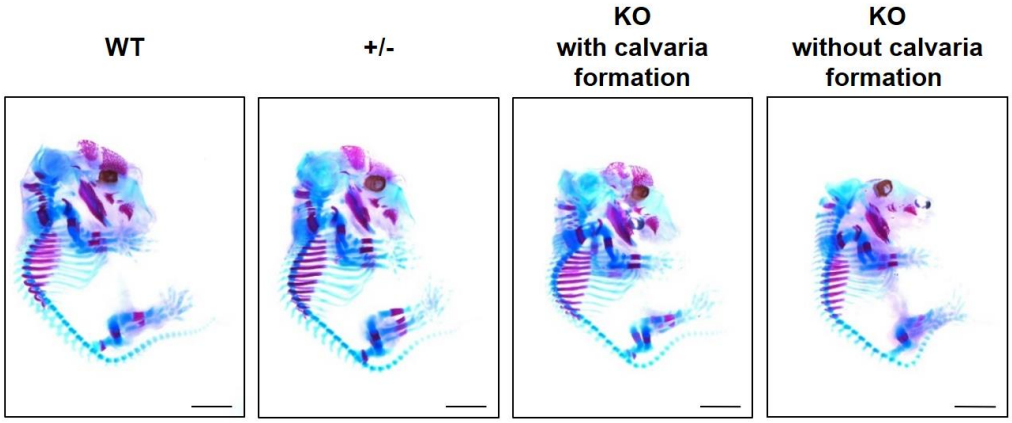

Fig. 2. Offspring genotypes from *Gnb1*-heterozygous intercrosses and phenotypes of skeletal structure from *Gnb1*-KO mice with and without calvaria formation.

(A) Percentage of offspring genotypes from *Gnb1* heterozygous intercrosses at E15.5. Percentage of the indicated phenotype in *Gnb1*-KO mice is shown in parentheses. (N = 124).

(B) Alizarin red and Alcian blue staining form skeletal preparation of E15 *Gnb1*-KO embryos with and without calvaria formation compared with heterozygous and WT littermates in lateral view. Scale bar, 2 mm.

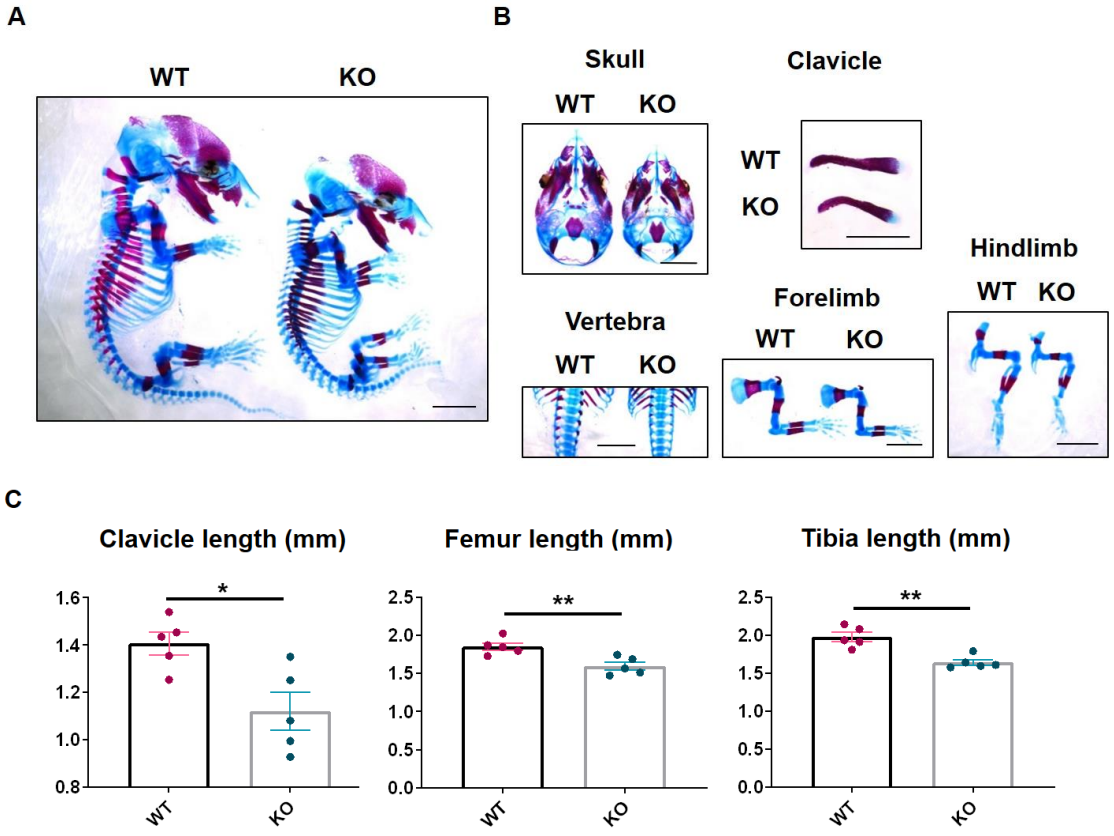

Fig. 3. Impaired skeletal development in *Gnb1*-KO mice.

(A) Alizarin red and Alcian blue staining form skeletal preparation of E15.5 *Gnb1*-KO and WT littermates in lateral view. Scale bar, 2 mm.

(B) Alizarin red and Alcian blue staining of the skull, clavicle, vertebra, forelimb, and hindlimb in *Gnb1*-KO and WT littermates shown in Fig. 3A. Scale bar, 2 mm for skull, vertebra, forelimb, and hindlimb. Scale bar, 1 mm for clavicle.

(C) Quantitative analysis of the length of clavicle, femur, and tibia from Alizarin red and Alcian blue stained *Gnb1*-KO and WT littermates at E15.5, assessed

under a stereo microscope (N = 5). Statistical analyses were performed by unpaired two-tailed Student's *t*-test. Data are shown as the mean ± SEM. *P < 0.05 vs. WT littermates. **P < 0.01 vs. WT littermates.

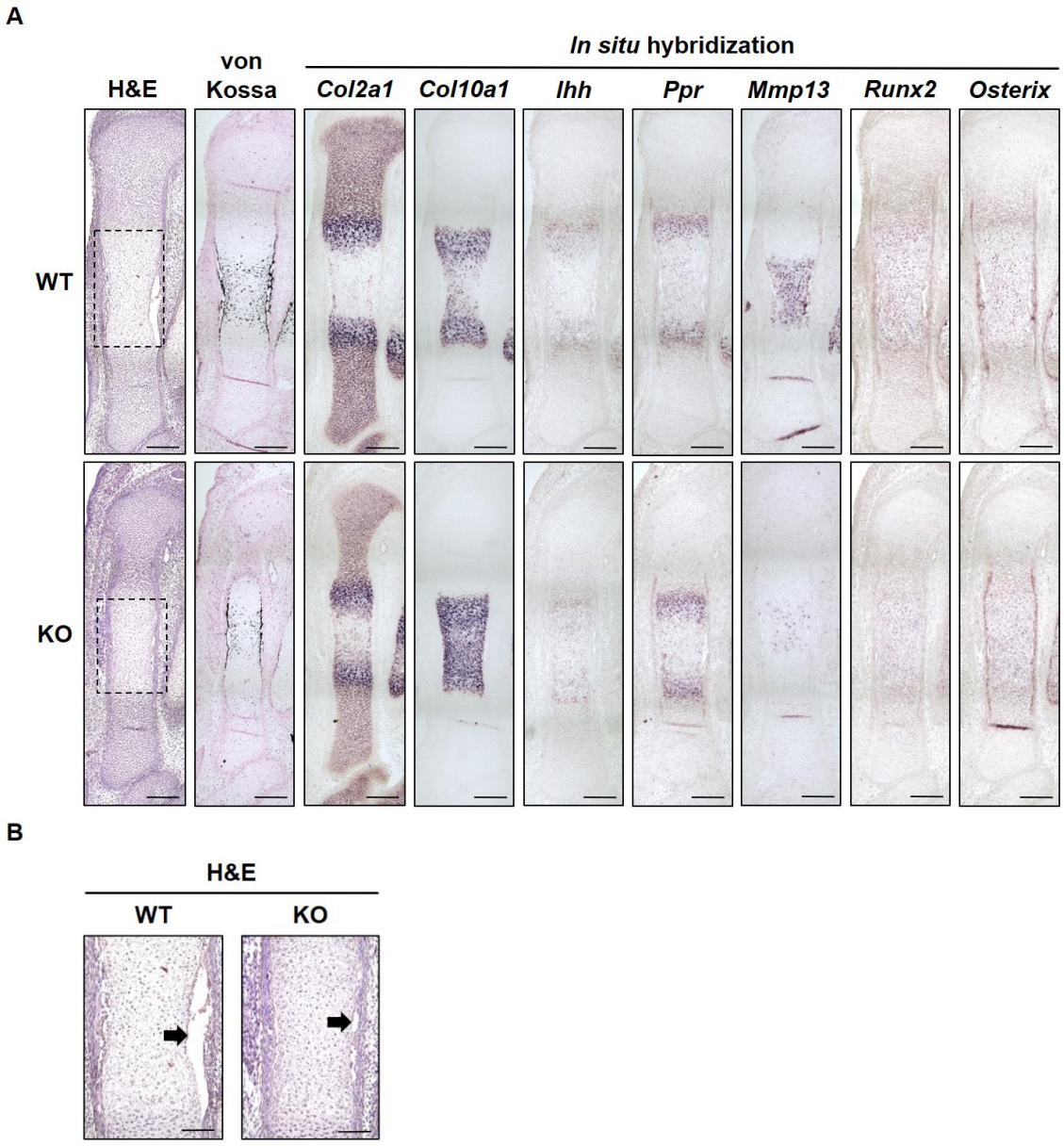

Fig. 4. The delay in the late stage of endochondral ossification in *Gnb1*-KO mice.

(A) H&E staining, von Kossa staining and *in situ* hybridization of paraffin sections from E15.5 tibia of *Gnb1*-KO and WT littermates. The boxed area in H&E staining

shows hypertrophic chondrocyte zone in *Gnb1*-KO and WT littermates. *In situ* hybridization probes are indicated. Scale bar, 200 μm.

(B) The higher magnification of hypertrophic chondrocyte zone from the boxed area in Fig. 4A. Arrows indicate space of vascular invasion. Scale bar, 100 μm.

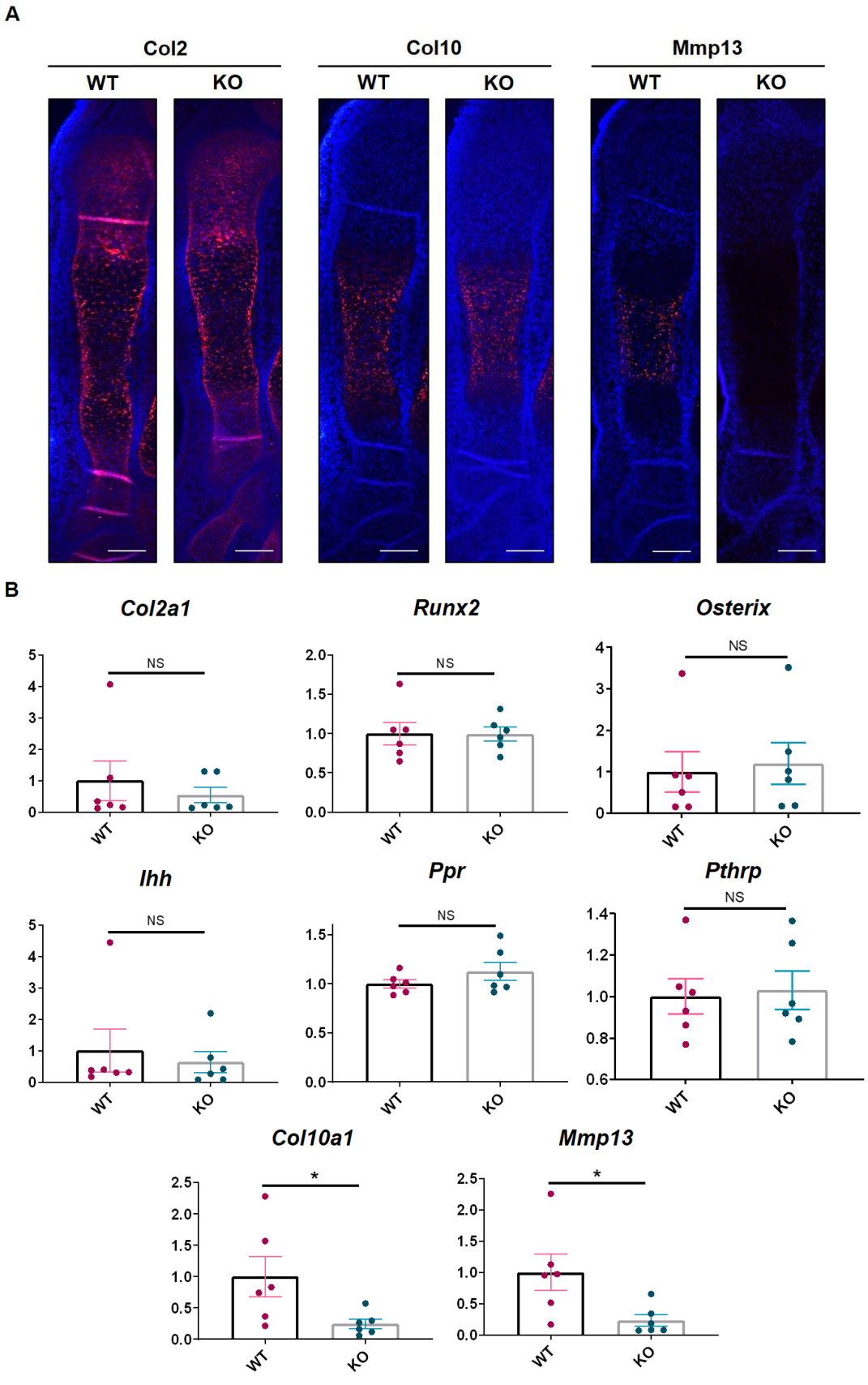
A
Col2
Col10
Mmp13
WT
KO
WT
KO
WT
KO
B
Col2a1
Runx2
Osterix
NS
NS
NS
Ihh
Ppr
Pthrp
NS
NS
NS
Col10a1
Mmp13
*
*
WT
KO

Fig. 5. Significant downregulation of *Col10a1* and *Mmp13* expression in *Gnb1* deficiency.

(A) The expression pattern of Col2, Col10, and Mmp13 in E15.5 tibia of *Gnb1*-KO and WT littermates from immunohistochemistry analysis using the specific antibodies. Blue indicates DAPI-stained nucleus. Scale bar, 200 μm.

(B) The mRNA expression of *Col2a1*, *Runx2*, *Osterix*, *Ihh*, *Ppr*, *Pthrp, Col10a1*, and *Mmp13* from RT-qPCR analysis. Total RNA was isolated from the hindlimbs of E15.5 *Gnb1*-KO and WT littermates (N = 6). Statistical analysis was performed by unpaired two-tailed Student's t-test. Data are shown as the mean ± SEM. *P < 0.05 vs. WT littermates. NS, not significant

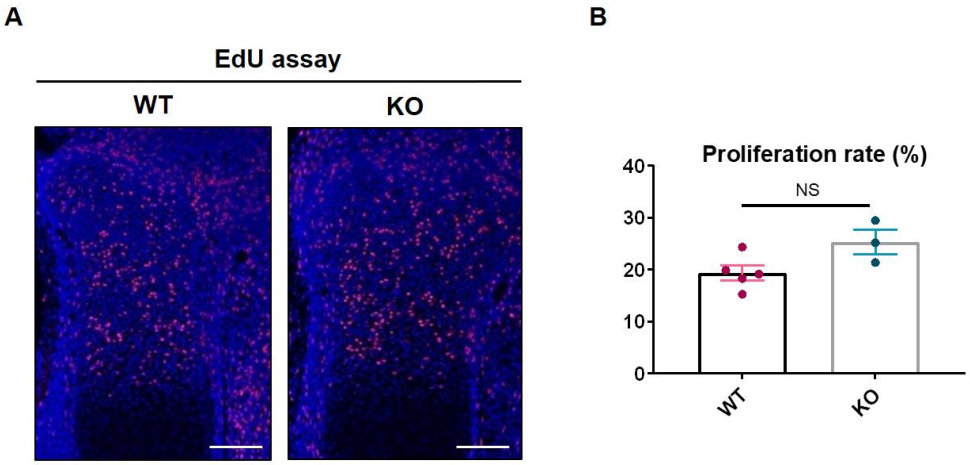

Fig. 6. Intact chondrocyte proliferation in absence of GNB1.

(A) *In vivo* EdU incorporation assay using *Gnb1*-KO and WT littermates at E15.5. Red indicates EdU positive nucleus and blue indicates DAPI-stained nucleus. Scale bar, 200 μm.

(B) Chondrocyte proliferation rate from quantitative analysis. The ratio of EdU positive nuclei to the total DAPI positive nuclei was calculated. (N = 5 for WT and N = 3 for KO). Statistical analysis was performed by unpaired two-tailed Student's t-test. Data are shown as the mean ± SEM. NS, not significant

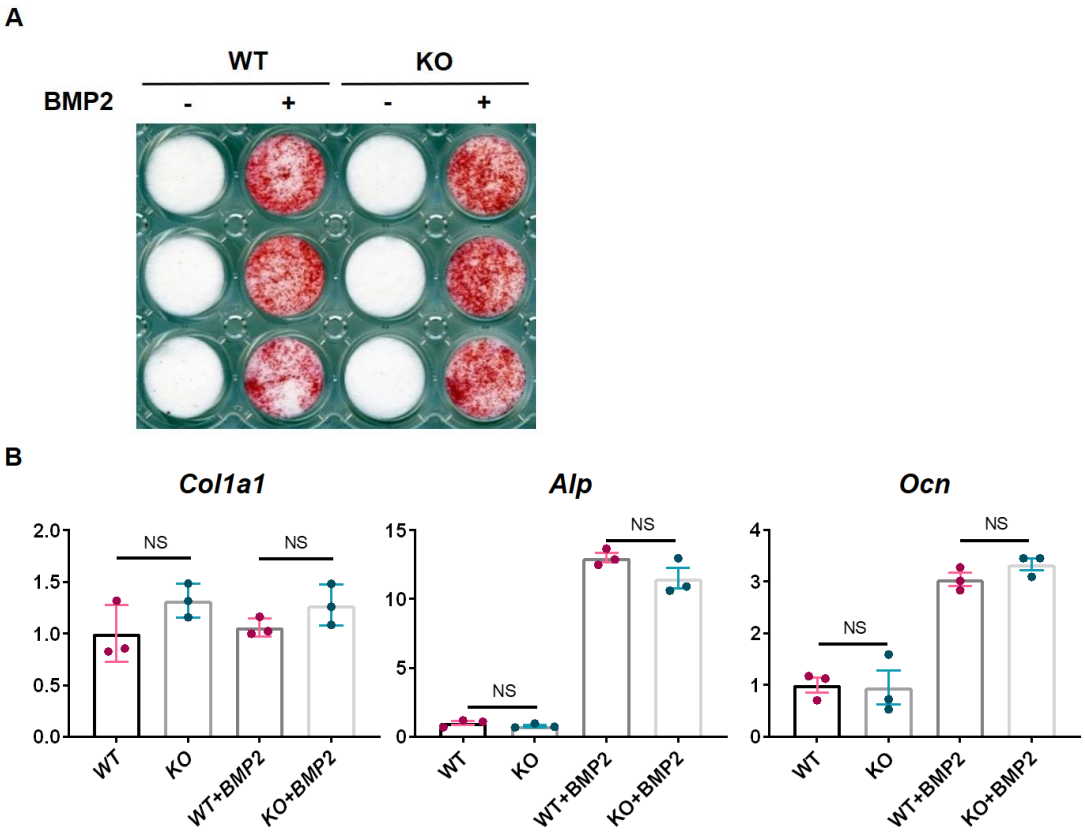

Fig. 7. Normal osteoblast differentiation and calcification in *Gnb1*-KO-derived osteoblasts.

(A) Alizarin red staining identified the osteoblastogenic and calcifying activities in primary osteoblast cultures. Primary osteoblasts isolated from calvariae of *Gnb1*-KO and WT littermates were grown to confluence and cultured in the absence or presence of BMP2 (100 ng/ml) for 6 days.

(B) RT-qPCR analysis showed mRNA expression of osteoblastic differentiation markers, *Col1a1*, *Alp*, and *Ocn* using the total RNA of primary osteoblasts

isolated from calvariae of *Gnb1*-KO and WT littermates (N = 3). Statistical analyses were performed by two-way ANOVA followed by Bonferroni *post hoc*-test. Data are shown as the mean ± SEM. NS, not significant.

Table 1. Primer sets used for RT-q

β-actin	sense: 5'-GGCTGTATTCCCCTCCATCG-3'
	antisense: 5'-CCAGTTGGTAACAATGCCATGT-3'
Col2a1	sense: 5'-CCTCCGTCTACTGTCCACTGAG-3'
	antisense: 5'-TGGAGCCCTGGATGAGCAAG-3'
Runx2	sense: 5'-CTCCTTCCAGGATGGTCCCA-3'
	antisense: 5'-CTTCCGTCAGCGTCAACACC-3'
Osterix	sense: 5'-AGCGACCACTTGAGCAAACAT-3'
	antisense: 5'-GCGGCTGATTGGCTTCTTCT-3'
Ihh	sense: 5'-GACTCATTGCCTCCCAGAACTG-3'
	antisense: 5'-CCAGGTAGTAGGGTCACATTGC-3'
Ppr	sense: 5'-TGCATATCATCGCGCAGGTG-3'
	antisense: 5'-GCCAGGAAGTAGAGGAAGAAGG-3'
Pthrp	sense: 5'-GAACATCAGCTACTGCATGACAAG-3'
	antisense: 5'-TCTGATTTCGGCTGTGTGGATC-3'
Col10a1	sense: 5'-GCCAAGCAGTCATGCCTGAT-3'
	antisense: 5'-GACACGGGCATACCTGTTACC-3'
Mmp13	sense: 5'-GGTTATGACATTCTGGAAGGTTATCC-3'
	antisense: 5'-CGTGGTTCTCAGAGAAGAAGAGG-3'
Col1a1	sense: 5'-GCAACAGTCGCTTCACCTACA-3'
	antisense: 5'-CAATGTCCAAGGGAGCCACAT-3'
Alp	sense: 5'-ATCTTTGGTCTGGCTCCCATG-3'
	antisense: 5'-TTTCCCGTTCACCGTCCAC-3'
Ocn	sense: 5'-GCAATAAGGTAGTGAACAGACTCC-3'
	antisense: 5'-GTTTGTAGGCGGTCTTCAAGC-3'